Supplementary information

Molecule-in-Memory: A Multiscale Guideline for Polymeric Tunnelling Layers Linking Molecular Motifs to Electrical Outcomes

Jin-Hyuk Kwon,[†a,b] Jeong-In Lee,[†c] Jonghee Lee,[a,c] Kenichi Chiba,[d] Yuji Shibasaki*[d] and Min-Hoi Kim*[a,c]

[a]Research Institute of Printed Electronics & 3D Printing, Industry University Cooperation Foundation, Hanbat National University, Daejeon 34158, Republic of Korea.

[b]Department of Electronics Engineering, Chungwoon University, Michuhol-gu, Incheon 22100, Republic of Korea.

[c]Department of Creative Convergence Engineering, Hanbat National University, Daejeon 34158, Republic of Korea.

[d]Department of Chemistry & Biological Sciences, Faculty of Science & Engineering, Iwate University, 4-3-5 Ueda, Morioka 020-8551, Japan.

*Correspondence: Yuji Shibasaki (Email: yshibasa@iwate-u.ac.jp), Min-Hoi Kim (Email: mhkim8@hanbat.ac.kr).

[†]These authors contributed equally to this work.

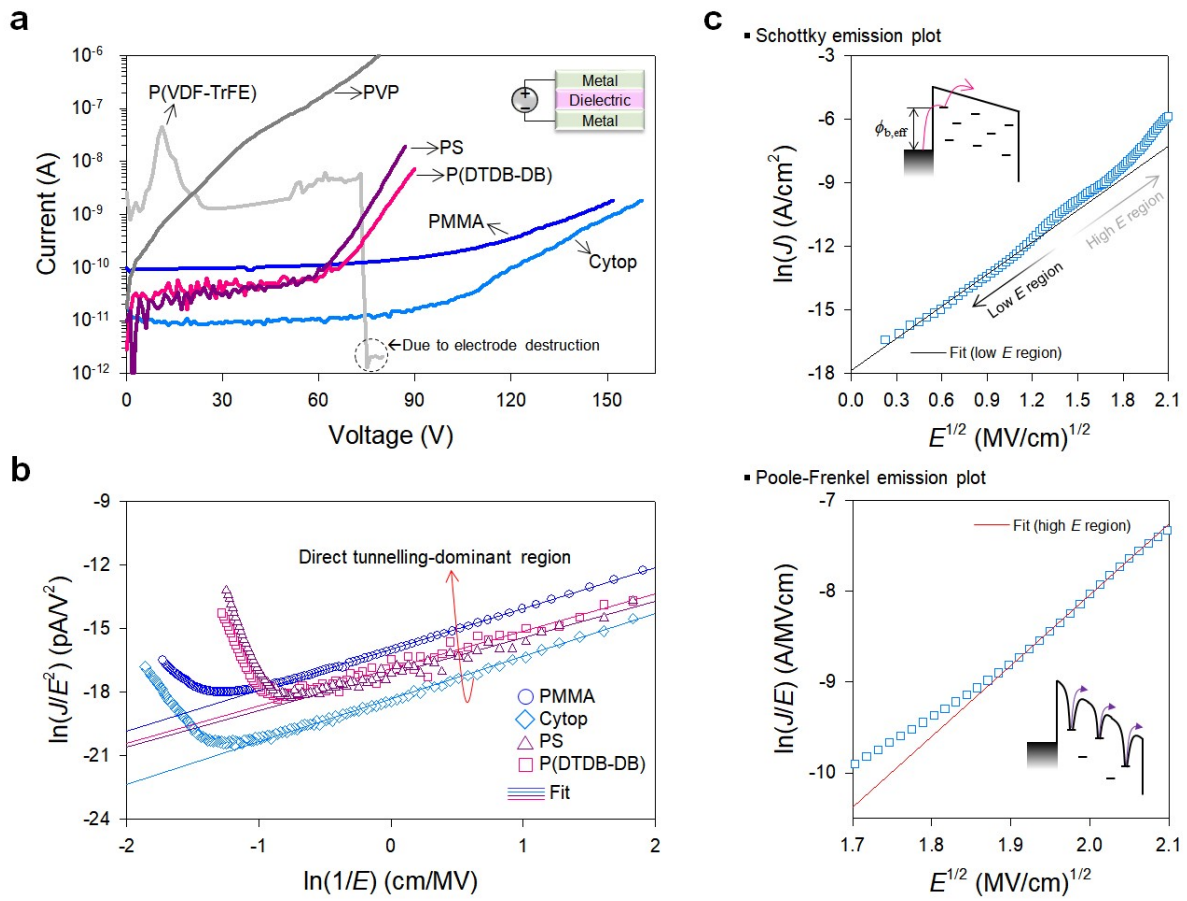

Figure S1. (**a**) Current-voltage characteristics of the MIM capacitors with PVP, P(VDF-TrFE), PMMA, Cytop, PS, and P(DTDB-DB) thin films as a function of the applied voltage, (**b**) $\ln(J/E^2)$ *vs*. $1/E$ plots of the PMMA, Cytop, PS, and P(DTDB-DB) capacitors, and (**c**) Schottky and Poole-Frenkel emission plots of the PVP capacitor.

The J_{leak} of the PVP capacitor was analyzed using the following relationships:

Schottky emission: $$J_S \propto exp\left(-\frac{\phi_b - \beta_S\sqrt{E}}{k_B T}\right) \quad (1)$$

Poole-Frenkel emission: $$J_{PF} \propto Eexp\left(-\frac{\phi_t - \beta_{PF}\sqrt{E}}{k_B T}\right) \quad (2)$$

where β_S and β_{PF} are constants. The Schottky and Poole-Frenkel emission plots exhibited linear behaviours in the low and high electric field regions, respectively (**Figure S1**c). Accordingly, Schottky emission is considered the dominant mechanism for the low-field conduction, while Poole-Frenkel emission dominates the high-field conduction. The Poole-Frenkel behaviour indicates a high density of charge traps, which is attributed to hydroxyl groups attached to the repeat units of PVP.

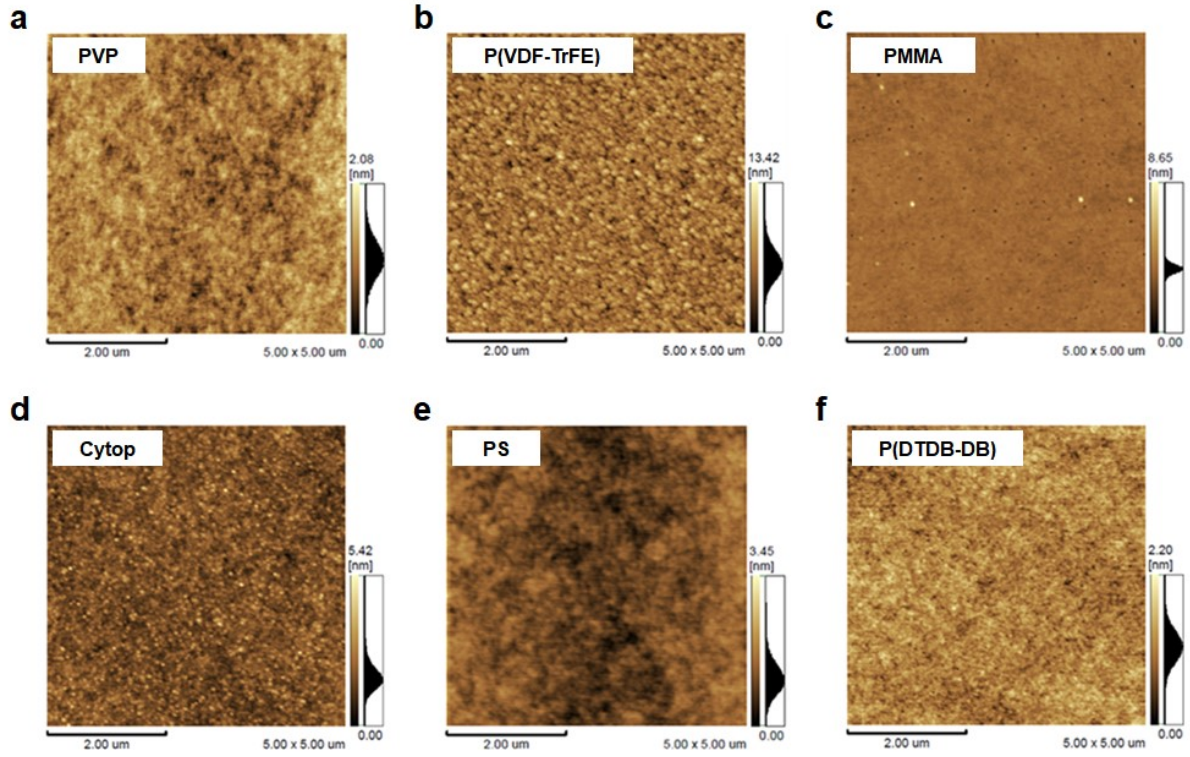

Figure S2. Atomic force microscopy images of (**a**) PVP, (**b**) P(VDF-TrFE), (**c**) PMMA, (**d**) Cytop, (**e**) PS, and (**f**) P(DTDB-DB) thin films.

The RMS surface roughness values of the PVP, P(VDF-TrFE), PMMA, Cytop, PS, and P(DTDB-DB) thin films were 0.2, 1.4, 0.2, 0.5, 0.3, and 0.2 nm, respectively.

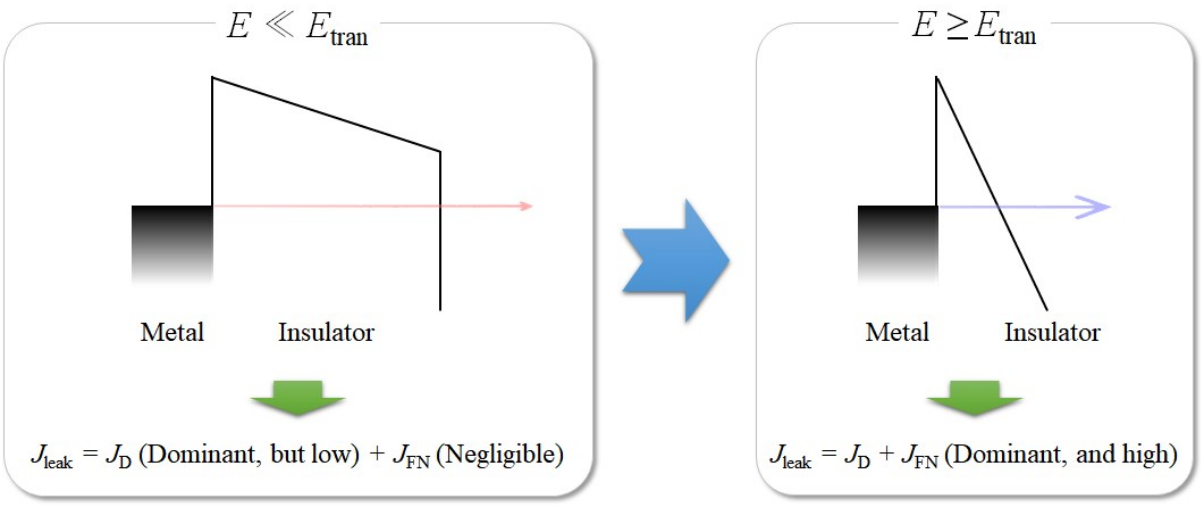

Figure S3. Conduction mechanism transition from direct tunnelling to FN tunnelling as a function of the applied electric field in the MIM capacitor (J_D: direct tunnelling current density).

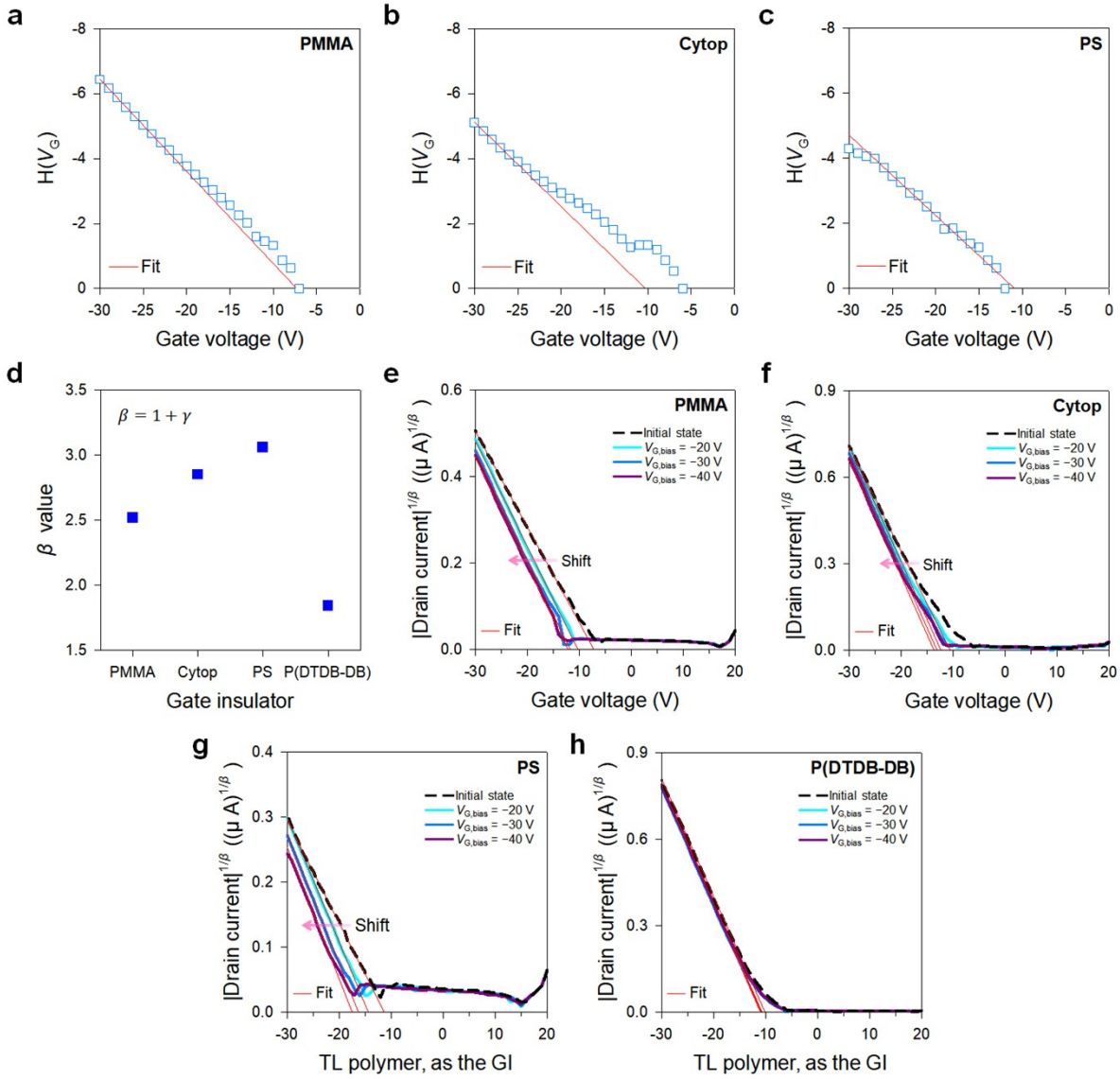

Figure S4. H-function analyses of the TFTs with (**a**) PMMA, (**b**) Cytop, and (**c**) PS as the GIs, (**d**) β values ($\beta = 1 + \gamma$), and $I_D^{1/\beta}$ *vs.* V_G plots of the transfer characteristic curves of the TFTs with (**e**) PMMA, (**f**) Cytop, (**g**) PS, and (**h**) P(DTDB-DB) as the GIs.

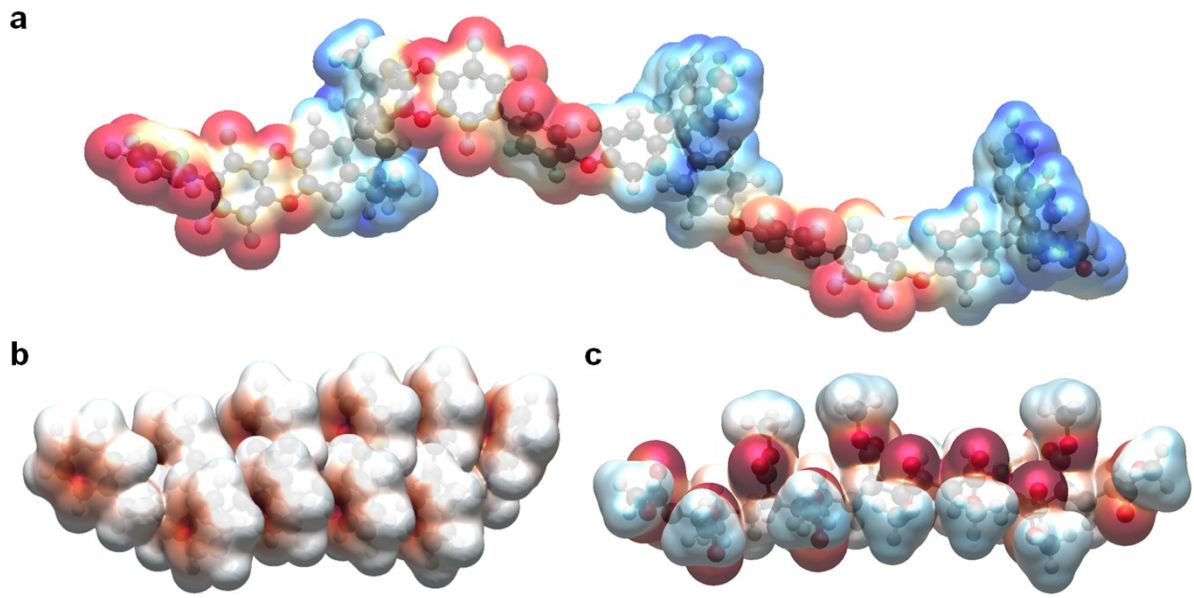

Figure S5. Electrostatic potential maps of partial P(DTDB-DB), PS, and PMMA structures, i.e., a 'DTDB-DB' structure, ten styrene units, and ten MMA units, respectively. Red and blue colors correspond to negative and positive electrostatic potential regions, respectively.

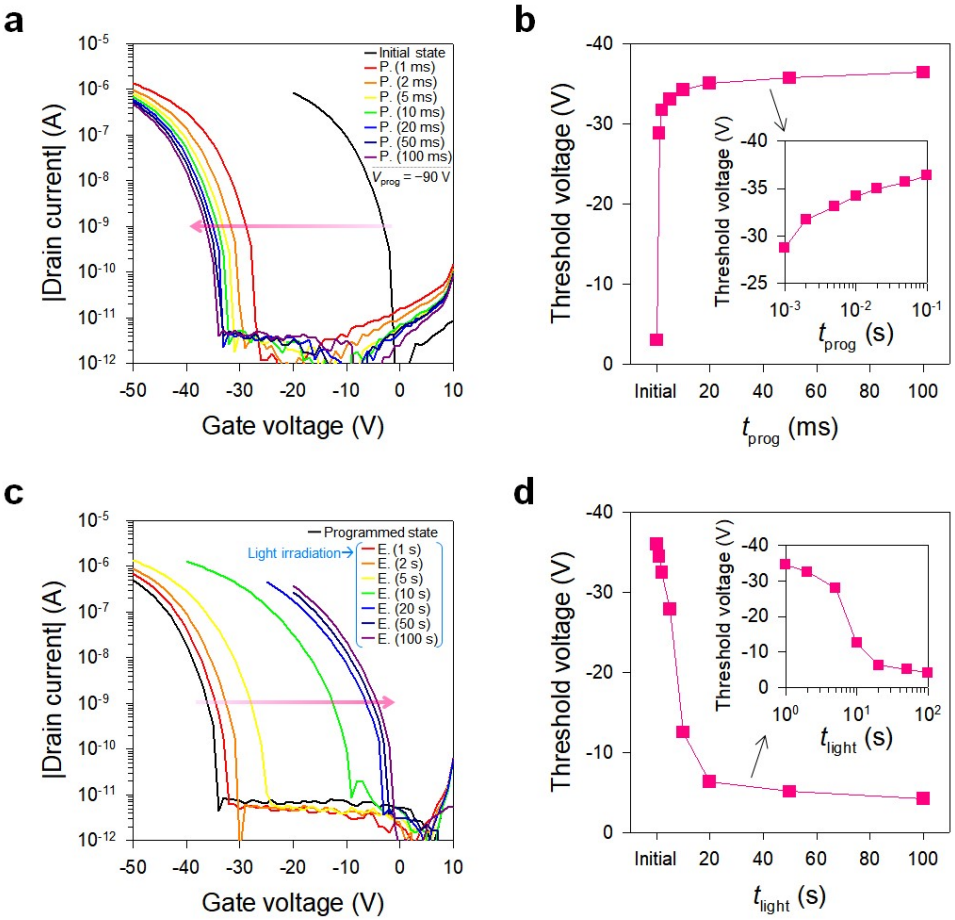

Figure S6. (**a**) Transfer characteristic curve shifts of the CTM with P(DTDB-DB) TL after program operations with V_{prog} = −90 V for 1, 2, 5, 10, 20, 50, and 100 ms and (**b**) corresponding V_{th} values as a function of the programming time. (**c**) Transfer characteristic curve shifts of the CTM with P(DTDB-DB) TL after erase operations with light irradiation (white light) for 1, 2, 5, 10, 20, 50, and 100 s and (**d**) corresponding V_{th} values as a function of the erasing time.

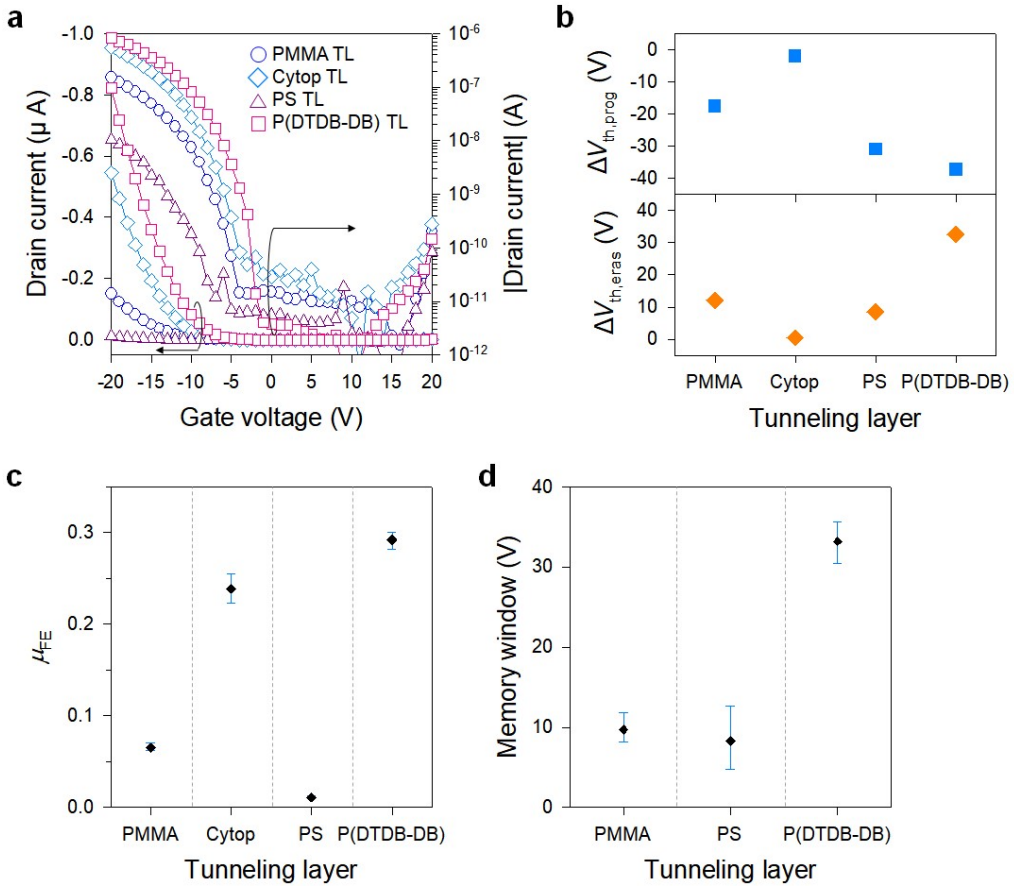

Figure S7. (**a**) Initial transfer characteristic curves of the CTMs with PMMA, Cytop, PS, and P(DTDB-DB) TLs at $V_D = -5$ V. (**b**) $\Delta V_{th,prog}$ and $\Delta V_{th,eras}$ values of the CTMs after a program operation with $V_{prog} = -90$ V (11 multiple pulses with a period of ~260 ms) and an erase operation with light irradiation (white light), respectively. (**c**) μ_{FE} (with error bars) and (**d**) memory window, i.e., $\Delta V_{th,eras}$ values (with error bars) of the CTMs with PMMA, Cytop, PS, and P(DTDB-DB) TLs.

The average μ_{FE} values of the CTMs with PMMA, Cytop, PS, and P(DTDB-DB) TLs were 0.065 ± 0.003, 0.239 ± 0.013, 0.011 ± 0.001, and 0.282 ± 0.019 cm^2/Vs, respectively. The average memory window, i.e., $\Delta V_{th,eras}$ values of the CTMs with PMMA, PS, and P(DTDB-DB) TLs were 9.7 ± 1.4, 8.3 ± 2.9, and 33.2 ± 1.7 V, respectively.

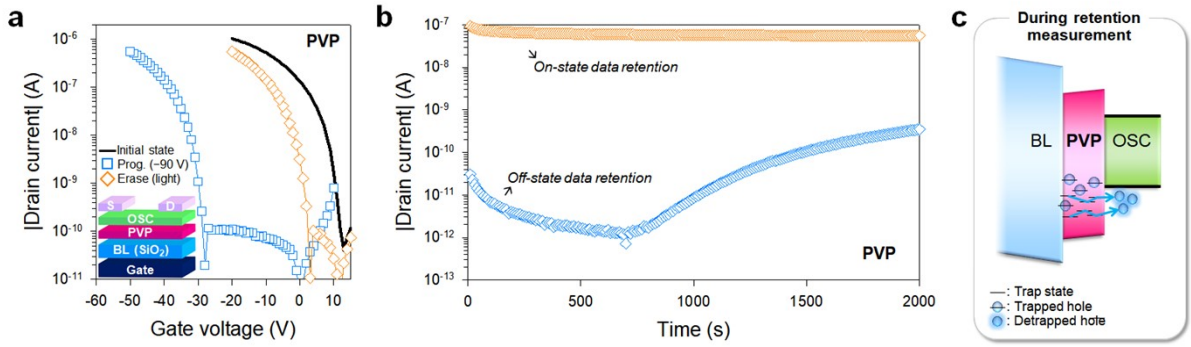

Figure S8. (**a**) Initial transfer characteristic curves of the CTM with a PVP layer at V_D = −5 V, and those measured after a program operation with V_{prog} = −90 V and an erase operation with light irradiation, (**b**) corresponding off-state and on-state data retention curves (at V_G = −10 V and V_D = −5 V), and (**c**) off-state data retention instability due to hole detrapping.

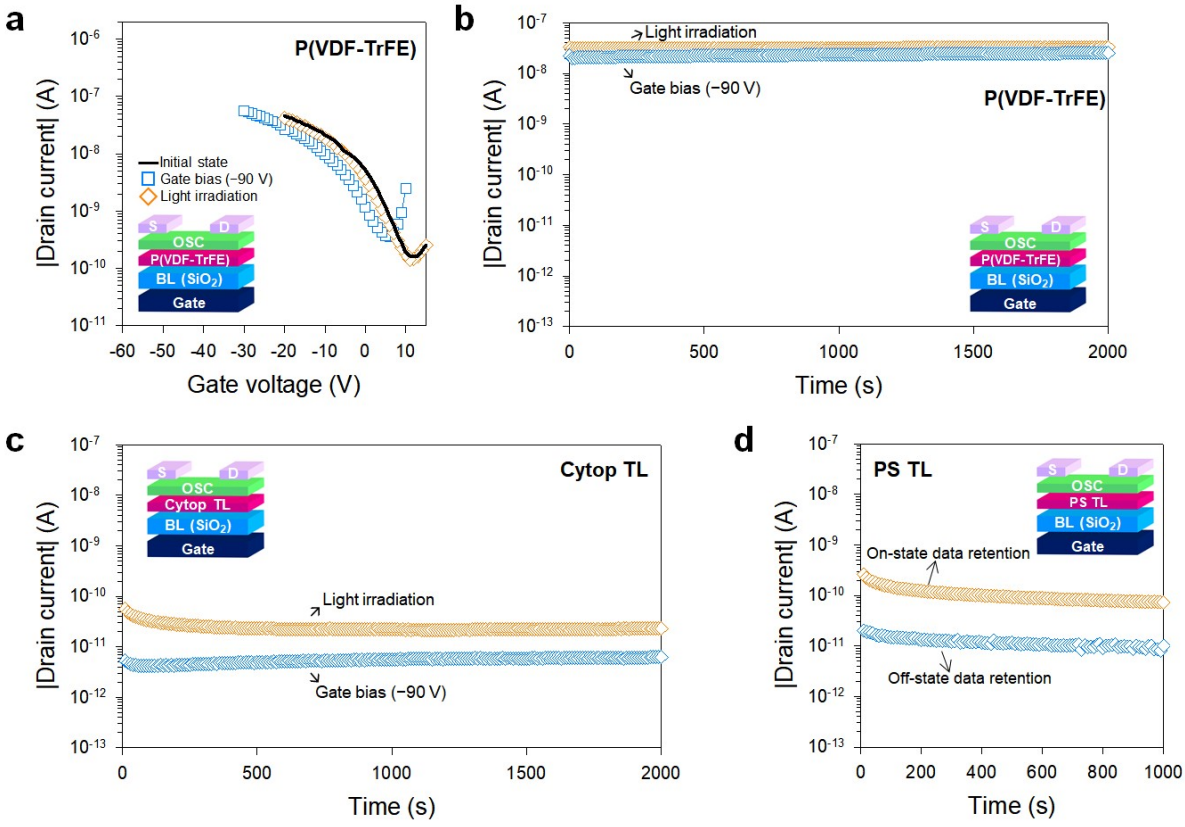

Figure S9. (**a**) Initial transfer characteristic curves of the CTM with a P(VDF-TrFE) layer, and those measured after the application of $V_{G,bias}$ = −90 V and after light irradiation, and (**b**) temporal I_D variations (at V_G = 5 V and V_D = −5 V) after the application of $V_{G,bias}$ = −90 V and after light irradiation (white light). (**c**) Temporal I_D variations of the CTM with a Cytop layer (at V_G = −5 V and V_D = −5 V) after the application of $V_{G,bias}$ = −90 V and after light irradiation. (**d**) Off-state and on-state data retention curves of the CTM with PS TL (at V_G = −36 V and V_D = −5 V) after programming with V_{prog} = −90 V (11 multiple pulses with a period of ~260 ms) and erasing with light irradiation (white light), respectively.

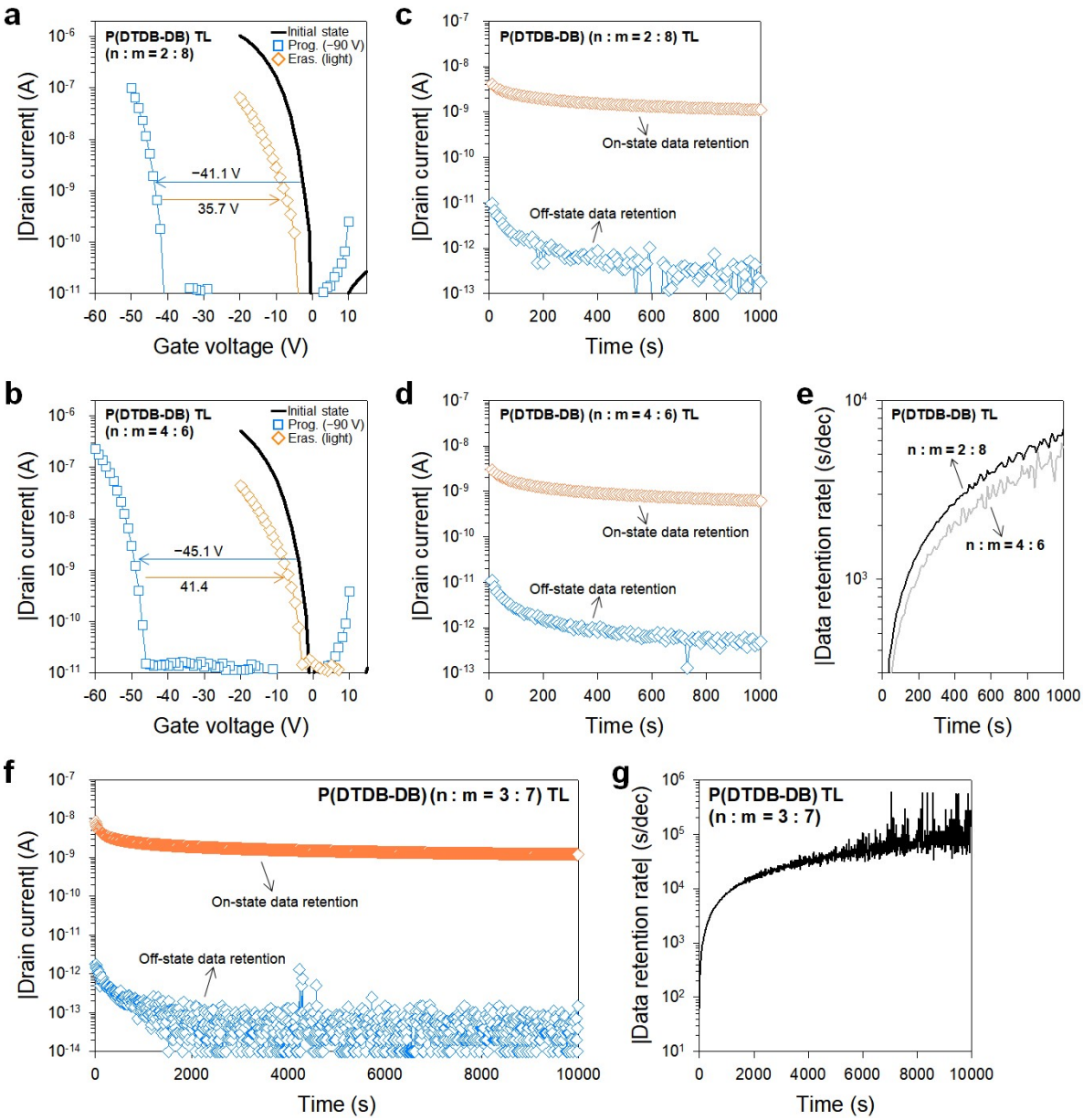

Figure S10. Initial transfer characteristic curves of the CTM with (**a**) n : m = 2 : 8 or (**b**) n : m = 4 : 6 P(DTDB-DB) TL at V_D = −5 V, and those measured after a program operation with V_{prog} = −90 V (11 multiple pulses with a period of ~270 ms) and an erase operation with light irradiation (white light), (**c**, **d**) its data retention curves (at V_G = −10 V and V_D = −5 V), and (**e**) R_{data} of the on-state data retention curve. (**f**) Data retention curves of the CTM with P(DTDB-DB) (n : m = 3: 7) TL (at V_G = −10 V and V_D = −5 V) after programming with V_{prog} = −90 V (11 multiple pulses with a period of ~260 ms) and erasing with light irradiation (white light), respectively, and (**g**) R_{data} of the on-state data retention curve.

When P(DTDB-DB) with n : m = 2 : 8 was used as the TL, the CTM exhibited memory characteristics

comparable to those of the CTM using P(DTDB-DB) with n : m = 3 : 7. However, the CTM using P(DTDB-DB) with n : m = 4 : 6 exhibited a slight increase in memory window, while showing relatively poor retention characteristics. The increase in memory window may be related to a reduction in the bandgap [1], which requires further investigation. In addition, such a trade-off relationship between memory window and data retention stability has also been reported in a previous study [2].

References

[1] Y. Konno, R. Osuga, J. N. Kondo, R. Ye, T. Tsukamoto, Y. Oishi and Y. Shibasaki, *Polymer*, 2021, **230**, 124072.

[2] S. P. Prakoso, H.-X. Peng, M.-N. Chen, Q.-A. Hong, R. Saleh and Y.-C. Chiu, *Adv. Funct. Mater.*, 2025, **35**, 2415415.

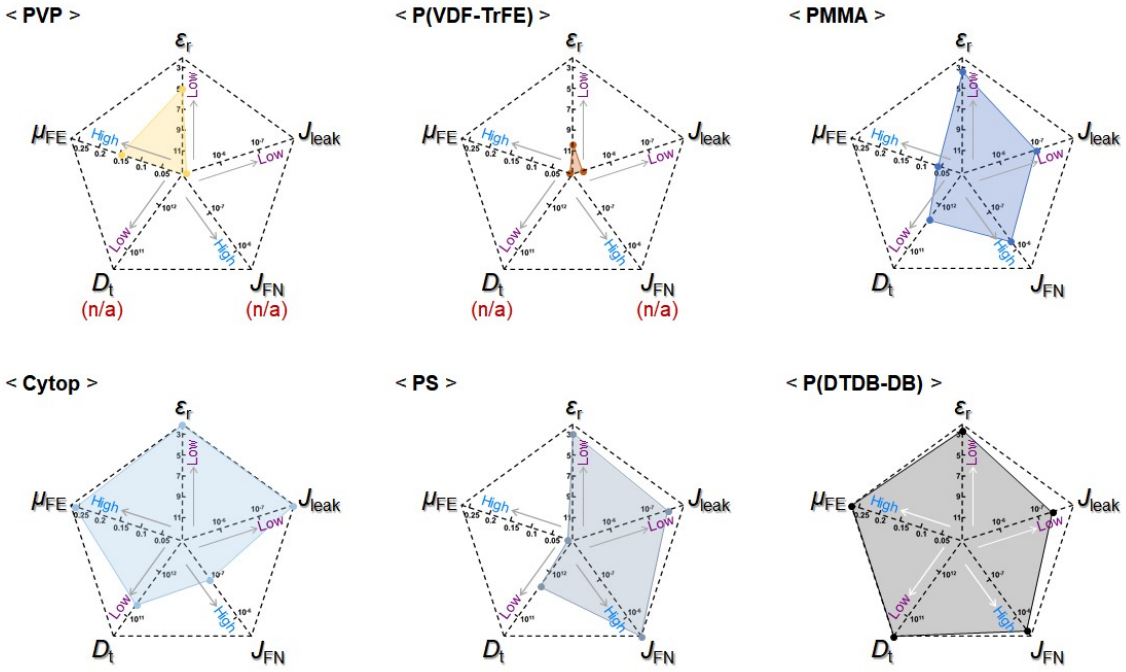

Figure S11. Radar charts displaying the ε_r, J_{leak}, J_{FN}, D_t, and μ_{FE} values obtained from PVP, P(VDF-TrFE), PMMA, Cytop, PS, and P(DTDB-DB).

● The ε_r values (at 1 kHz) of PVP, P(VDF-TrFE), PMMA, Cytop, PS, and P(DTDB-DB) are 5.0, 10.2, 3.4, 2.1, 2.9, and 2.6, respectively.

● The average J_{leak} values of the PVP, P(VDF-TrFE), PMMA, Cytop, PS, and P(DTDB-DB) capacitors, calculated over the electric-field range from 0 to 2 MV/cm, are 7.7×10^{-6}, 5.5×10^{-6}, 1.1×10^{-7}, 1.1×10^{-8}, 3.0×10^{-8}, and 4.1×10^{-8} A/cm^2, respectively.

● The average J_{FN} values of the PMMA, Cytop, PS, and P(DTDB-DB) capacitors, calculated over the electric-field range from each E_{tran} to E_{tran} + 0.8 MV/cm, are 6.2×10^{-7}, 1.0×10^{-7}, 3.2×10^{-6}, and 2.3×10^{-6} A/cm^2, respectively.

● The D_t values for PMMA, Cytop, PS, and P(DTDB-DB), after the stress application with $V_{G,bias} = -40$ V, are 4.7×10^{11}, 1.8×10^{11}, 5.0×10^{11}, and 3.6×10^{10} cm^{-2}, respectively.

● The μ_{FE} values of the CTMs with PVP, P(VDF-TrFE), PMMA, Cytop, PS, and P(DTDB-DB) are 0.15, 0.01, 0.06, 0.26, 0.01, and 0.27 cm^2/Vs, respectively.